Hindawi Publishing Corporation
International Journal of Antennas and Propagation
Volume 2008, Article ID 384792, 6 pages
doi:10.1155/2008/384792

Research Article

Accurate Analysis of Practical 3D Periodic Leaky-Wave Patch Antennas

Mohammad R. Zunoubi and Hassan A. Kalhor

Electrical and Computer Engineering Department, State University of New York, 1 Hawk Drive, New Paltz, NY 12561, USA

Correspondence should be addressed to Mohammad R. Zunoubi, zunoubm@engr.newpaltz.edu

Received 23 March 2007; Revised 8 November 2007; Accepted 4 February 2008

Recommended by Miguel Ferrando

This paper presents a new analysis method based on the finite integral technique (FIT) of practical three-dimensional leaky-wave antennas comprised of a finite number of patches arranged in arrays. Radiation patterns and scattering parameters are calculated and compared with corresponding measured results to demonstrate the adequacy and the accuracy of the proposed method. The technique is then used as an antenna design tool to obtain the desired radiation patterns and beam scanning by selective choice of array elements dimensions, spacing, and substrate parameters.

1. INTRODUCTION

The foundation for surface-wave andleaky-wave antennas was laid by Sommerfeld in 1899 [1]. After this pioneering work, leaky-wave antennas (LWAs) have been the subject of many investigations [2, 3]. The planar printed-circuit leaky-wave antenna arrays with discrete periodic energy leakage have, however, been the focus of research in recent years [4, 5]. The interest in these newer antenna types stems from their ability to produce both broadside pencil beams and scanned conical beams, and their structural simplicity such as low-profile construction and ease of integration with other planar structures. The beam scanning ability of early leaky-wave antennas was achieved by using substrates with dielectric materials of permittivity as high as 100 which were clearly not realistic [6, 7]. Alternatively, the idea of using multilayered dielectric substrates was introduced which used lower permittivity but added significant complexity to the theoretical analysis and antenna fabrication [8]. Later, Zhao et al. reported a new planar structure that consisted of infinite periodic arrays of metallic patches separated from a ground plane by substrates that had lower dielectric permittivity, which permitted beam scanning from broadside to close to end-fire by adjusting other antenna parameters [9]. Their analysis was based on a method of moments approach along with the application of reciprocity theorem to obtain the far-field patterns of a short electric dipole positioned in the middle of the dielectric substrate. Instead of the actual radiation problem, they calculated the scattering of the entire structure under plane wave illumination. Although their contribution offers major insights into the operation of periodic planar leaky-wave antennas, their approach is limited to 2-dimensional infinite structures. The analysis of practical antennas with finite number of elements is substantially more difficult.

The purpose of this research is to present a complete analysis and design of 3-dimensional finite periodic planar leaky-wave patch antennas which have practical significance. Such structure is seen in Figure 1.

The patch antenna consists of a simple finite periodic planar array of metal strips that are printed on a grounded dielectric substrate as depicted above. A small horizontal dipole located in the middle of the substrate with a length of l_d is used as the source in modeling because it is easy to analyze and launche the desired leaky waves on the antenna. In experimental verifications, more convenient methods of excitation may be used without changing the antenna pattern appreciably. In our measurements, we employed a coaxial line that was insulated from and passed through the ground plane and fed the horizontal dipole antenna. The inner conductor was connected to one arm, and the outer conductor was shorted to the second arm of the dipole. Also as shown in Figure 1, w and l are the width and length of array patches, a and b are their periodicities in x and

y directions, respectively, and h is the substrate thickness. The finite integration technique (FIT) [10] and perfectly matched layer (PML) absorbing boundary condition [11] are combined in a numerical technique introduced earlier by the authors to analyze general diffraction gratings [12] and periodic slot antennas [13]. This method is now extended, specialized, and used to solve the present finite periodic patch antenna to obtain convergent and accurate results. The main contribution of this work is that it analyzes a practical finite size antenna which is analytically more demanding than an idealized infinite structure in which infinite periodicity can be used to advantage. Different parameters including substrate height and permittivity, the patch width w and length l, the periodicities a and b, and the frequency are varied to investigate the effects on the antenna scanning properties and to obtain patterns that may be either a pencil beam at broadside, or a conical beam, depending on the desired scan angle. The results are cast into a few empirical design equations that can serve as convenient design tools.

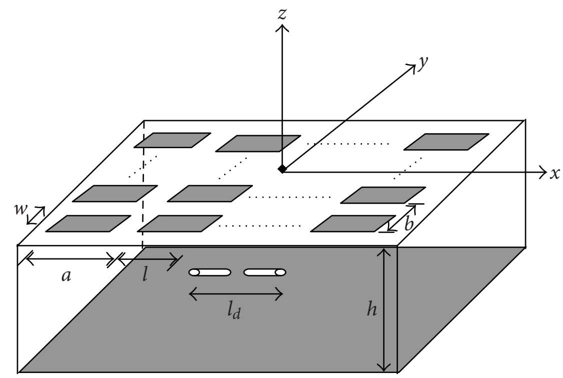

Figure 1: The geometry of the practical printed-circuit leaky-wave periodic patch antenna.

2. FORMULATION

One of the direct methods of solving Maxwell's equations is the finite integration technique (FIT) that is based on the integral form of these equations which are

$$\oint_c \vec{E}(\vec{r},t)\cdot d\vec{l} = -\iint_s \frac{\partial}{\partial t}\vec{B}(\vec{r},t)\cdot d\vec{s}, \qquad (1)$$

$$\oint_c \vec{H}(\vec{r},t)\cdot d\vec{l} = \iint_s \left\{\frac{\partial}{\partial t}\vec{D}(\vec{r},t) + \vec{J}(\vec{r},t)\right\}\cdot d\vec{s}, \qquad (2)$$

$$\oiint_s \vec{D}(\vec{r},t)\cdot d\vec{s} = 0, \qquad (3)$$

$$\oiint_s \vec{B}(\vec{r},t)\cdot d\vec{s} = 0\ . \qquad (4)$$

These equations are discretized by first defining a grid cell complex G as

$$G = \{V_{i,j,k} \in R^3 \mid V_{i,j,k} := [x_i, x_{i+1}]\times[y_j, y_{j+1}]\times[z_k, z_{k+1}]\},$$
$$i = 1,\ldots,I-1,\ j = 1,\ldots,J-1,\ k = 1,\ldots,K-1. \qquad (5)$$

Faraday's law of (1) is then discretized on a cell $V_{i,j,k}$ of G according to

$$\widehat{e}_x(i,j,k) + \widehat{e}_y(i+1,j,k) - \widehat{e}_x(i,j+1,k) - \widehat{e}_y(i,j,k) = -\frac{d}{dt}\widehat{\widehat{b}}_z(i,j,k), \qquad (6)$$

where $\widehat{e}_x(i,j,k) = \int_{(x_i,y_j,z_k)}^{(x_{i+1},y_j,z_k)} \vec{E}\cdot d\vec{l}$ is the voltage along one edge of surface $S_z(i,j,z)$ and $\widehat{\widehat{b}}_z(i,j,k) = \int_{s_z(i,j,k)} \vec{B}\cdot d\vec{s}$ is the magnetic flux through the cell face $S_z(i,j,z)$ as shown in Figure 2. The above procedure is carried out over all grid surfaces of G to obtain the matrix equation:

$$C\,\widehat{e} = -\frac{d}{dt}\widehat{\widehat{b}}, \qquad (7)$$

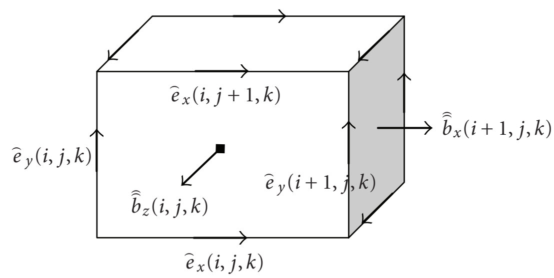

Figure 2: Electric voltages and magnetic flux allocations on a cell $V_{i,j,k}$.

where C is the discrete curl matrix, $\widehat{e}$ is the vector containing electric voltages, and $\widehat{\widehat{b}}$ is the magnetic flux vector. The magnetic Gauss's law of (4) is then discretized by performing the surface integral over the six faces of the cell shown in Figure 2 to obtain

$$-\widehat{\widehat{b}}_x(i,j,k) + \widehat{\widehat{b}}_x(i+1,j,k) - \widehat{\widehat{b}}_y(i,j,k) + \widehat{\widehat{b}}_y(i,j+1,k) - \widehat{\widehat{b}}_z(i,j,k) + \widehat{\widehat{b}}_z(i,j,k+1) = 0. \qquad (8)$$

Upon applying the above discretization to all grid volumes of G, the following matrix equation is obtained:

$$S\widehat{\widehat{b}} = 0 \qquad (9)$$

with S being the discrete divergence matrix.

Ampere's law of (2) and the electric Gauss's law of (3) are discretized in a similar manner using a dual grid $\widetilde{G}$ with foci of G as its grid points to obtain the corresponding matrix equations:

$$\widetilde{C}\,\widehat{h} = \frac{d}{dt}\widehat{\widehat{d}} + \widehat{j}, \qquad \widetilde{S}\widehat{\widehat{d}} = q. \qquad (10)$$

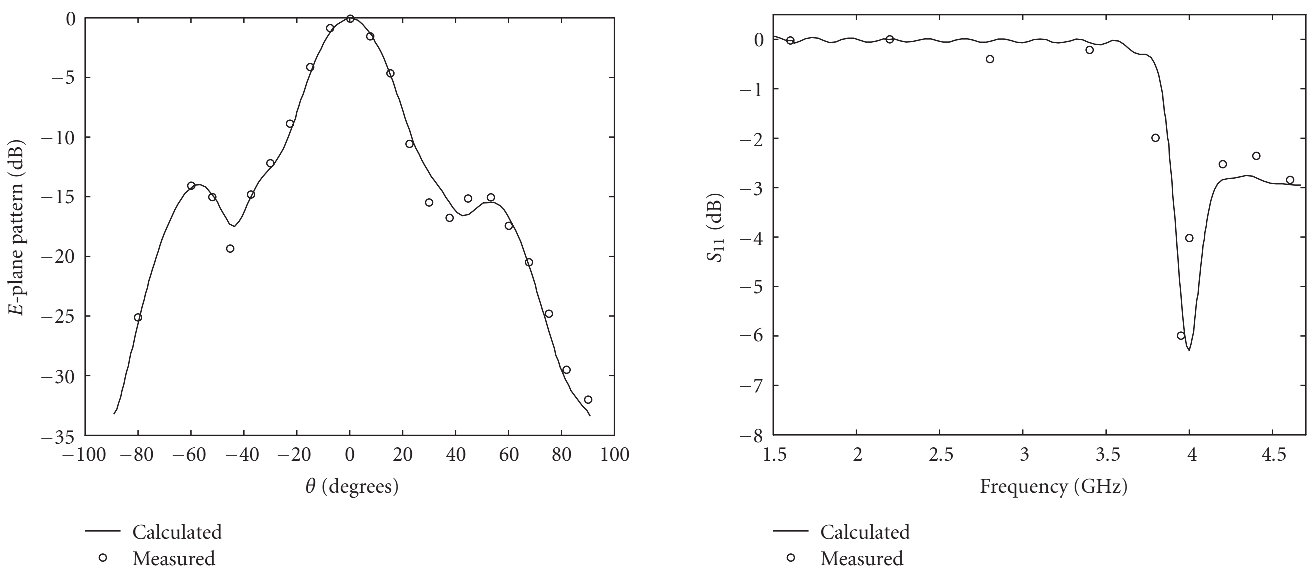

(a) E-plane pattern calculated and measured at 4 GHz

(b) A comparison of the calculated and measured S_{11}

Figure 3

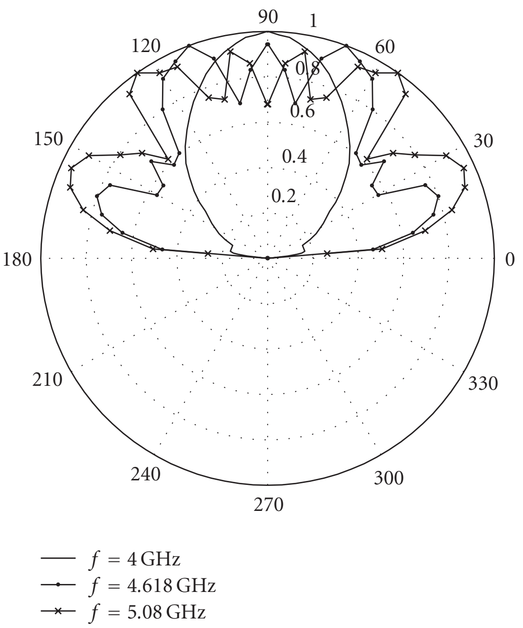

Figure 4: E-plane pattern for $f = 4.0$, 4.618, and 5.08 GHz.

As the final step, the following equations involving constitutive parameters are used to relate the integral of the voltage and flux state variables allocated on G and $\widetilde{G}$:

$$\widehat{d} = M_{\varepsilon}\widehat{e} + \widehat{\widehat{p}}, \qquad \widehat{\widehat{j}} = M_{\kappa}\widehat{e}, \qquad \widehat{h} = M_{\nu}\widehat{\widehat{b}} - \widehat{m}, \tag{11}$$

where $M_{\varepsilon}, M_{\kappa},$ andM_{ν} are the permittivity, conductivity, and reluctivity matrices, respectively, and $\widehat{\widehat{p}}$ and $\widehat{m}$ are permanent electric and magnetic polarizations. Additionally, the time derivatives in (7) and (10) are discretized through application of a simple forward difference scheme as

$$\frac{d}{dt}\widehat{\widehat{b}}_z(i,j,k) = \frac{\widehat{\widehat{b}}_z^{\,n-1/2}(i,j,k) - \widehat{\widehat{b}}_z^{\,n+1/2}(i,j,k)}{\Delta t}, \tag{12}$$

Δt is the time step chosen to satisfy the Courant stability criterion.

3. RESULTS

We first illustrate the accuracy and effectiveness of our numerical implementation by calculating the radiation pattern and S_{11} parameter of a 9×9 periodic planar patch antenna and comparing the results with their corresponding measured values. Antenna parameters are selected to obtain a broadside pencil beam pattern. Referring to the antenna geometry shown in Figure 1, the following parameters are chosen: $a = 0.54\,\lambda$, $b = 0.12\,\lambda$, $w = 0.04\,\lambda$, $l = 0.5\,\lambda$, $h = 0.5333\,\lambda$, $\varepsilon_r = 1.0$, and an operating frequency of $f_r = 4$ GHz. The leaky waves are excited by an x-directed infinitesimal dipole antenna of length $l_d = 0.1\,\lambda$ located at the middle of the substrate and the E-plane radiation pattern ($\varphi = 0^\circ$) and the S_{11} parameter are calculated and compared with the measured results. The comparisons are seen in Figure 3 and indicate excellent agreements.

After the accuracy of our numerical implementation is verified, we first investigate the effect of changing the operating frequency on the radiation property of the antenna with its parameters described above. The frequencies of 4.0 GHz, 4.618 GHz, and 5.08 GHz are considered. As seen in Figure 4, the resulting radiation patterns are broadside for $f_r = 4.0$ GHz and scans to 25° and 40° at the two higher frequencies.

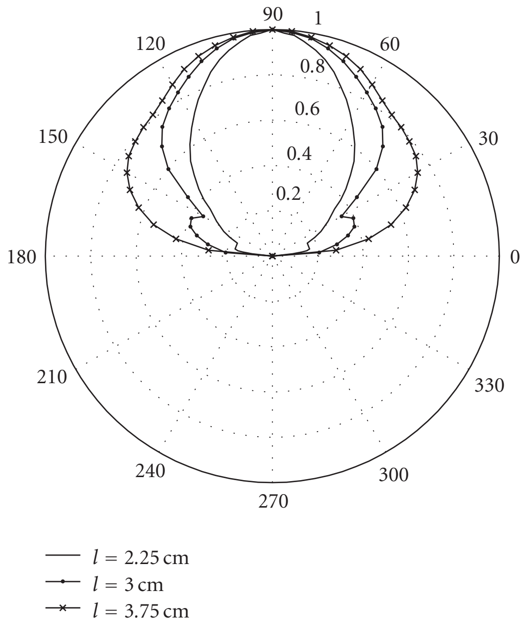

Figure 5: E-plane pattern for l = 2.25, 3.0, and 3.75 cm.

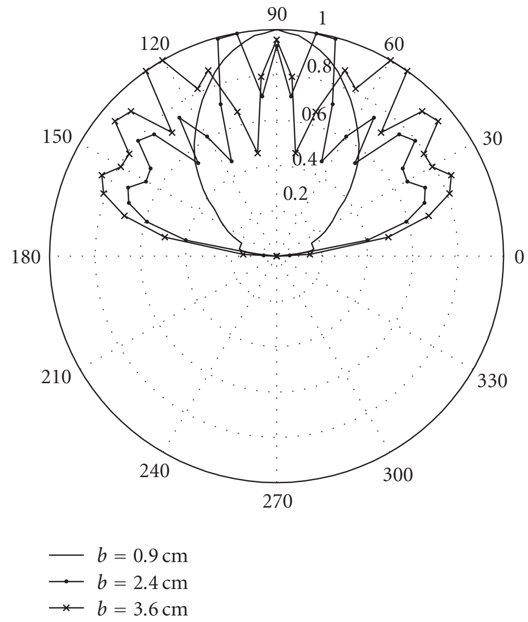

Figure 6: E-plane patterns for b = 0.9, 2.4, and 3.6 cm.

The next study focuses on the variation of the strip length l. As seen in Figure 5, the patterns become broader as l decreases from 3.75 cm to 3.0 cm and 2.25 cm (corresponding to 0.5 λ, 0.4 λ, and 0.3 λ) supporting the fact that the patch arrays are not confining the leaky waves and the patterns become closer to the pattern of a simple short electric dipole.

In order to study the effects of changing the periodicity of the arrays in the y direction on the patterns, we compute patterns for b of 0.9 cm, 2.4 cm, and 3.6 cm (corresponding to 0.12 λ, 0.32 λ, and 0.48 λ). Results are shown in Figure 6 and indicate that the main beam scans from broadside to 15° and 33°, respectively, illustrating the scanning capability of the structure.

We then investigate the effect of substrate height on the radiation property of the antenna at h of 3.99 cm, 4.63 cm, and 5.7 cm. It is seen in Figure 7 that the resulting radiation pattern is broadside for $h = 3.99$ cm, and then it scans to 25°, and 37° as h varies from 4.63 cm to 5.7 cm.

The last study involves varying the substrate permittivity from air, $\varepsilon_r = 1$ to 1.1, and 2.2 and calculating the far-field patterns of the antenna. The simulation results are shown in Figure 8, where it is observed that as the permittivity increases from 1 to 1.1, the main lobe scans from broadside pencil beam to 12°. However, for $\varepsilon_r = 2.2$, the pattern is degraded which is consistent with the results reported in [9].

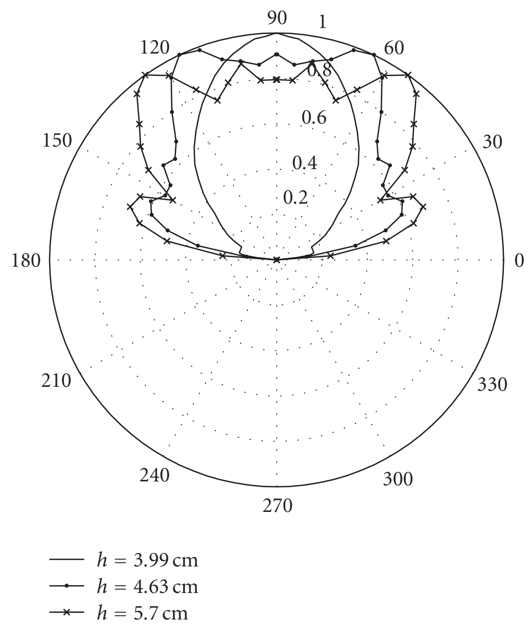

Figure 7: E-plane patterns for h = 3.999, 4.63, and 5.7 cm.

4. DESIGN RULES

In this section, we use our numerical results presented above to obtain empirical equations that can serve as convenient design tools for finite arrays of leaky-wave patch antennas.

4.1. Substrate height

Based on the results shown in Figures 6 and 7, we have found that for a finite structure of 9 × 9 patch antenna, the substrate thickness h is related to the scan angle θ_p by

$$\frac{h}{\lambda_0} = \frac{0.58}{\sqrt{\varepsilon_r - \sin^2\theta_p}}, \tag{13}$$

where λ_0 is the free-space wavelength and ε_r is the substrate relative permittivity. For the infinite structure operating in

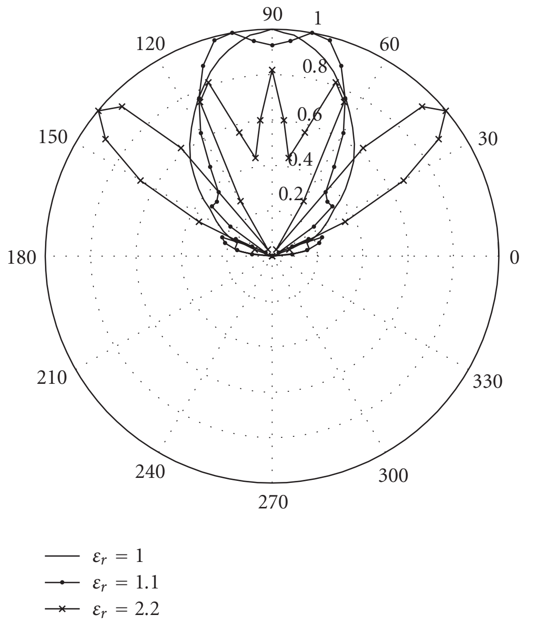

Figure 8: E-plane patterns for $\varepsilon_r = 1.0$, 1.1, and 2.2.

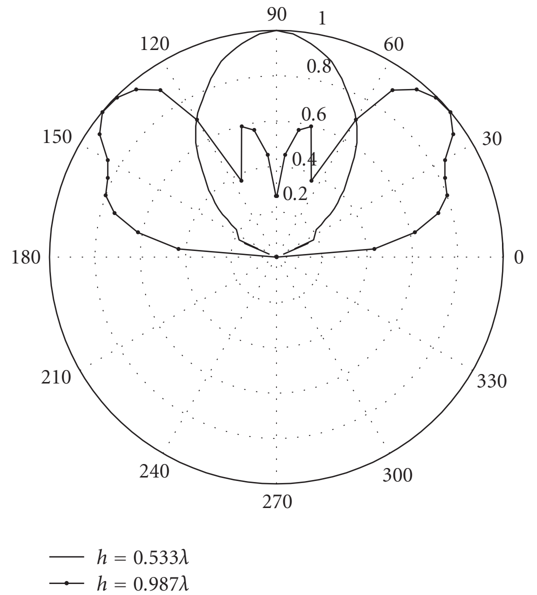

Figure 9: E-plane patterns for $\varepsilon_r = 1.0$, $h = 0.533\ \lambda$, and $h = 0.987\ \lambda$.

the order 1 mode, the theoretical value of the coefficient in (13) is 0.58 instead of 0.5 [9].

4.2. *Operating frequency*

According to (13), with a fixed substrate height h, a desired scan angle θ_p can be obtained by varying the frequency. The results in Figure 4 show that as the frequency increases,the scan angle increases as predicted by (13).

4.3. *Maximum scan angle with a single beam*

It is known that for mode $n = 2$ to radiate at broadside, the substrate height h should be [9]

$$\frac{h}{\lambda_0} = \frac{1.0}{\sqrt{\varepsilon_r}}. \tag{14}$$

However, for this substrate thickness, the scan angle for $n = 1$ mode can be written based on (13) as

$$\theta_p = \sin^{-1}\frac{\sqrt{1.973\varepsilon_r}}{1.724} = \sin^{-1}\left[0.814\sqrt{\varepsilon_r}\right]. \tag{15}$$

Therefore, (15) should provide the maximum possible angle for single mode operation without degradation from the higher-order modes. Based on (15), for an air-filled substrate, the maximum scan angle should be 54°. When this value is used in (13), a substrate thickness of 0.987 λ_0 is obtained. To illustrate the accuracy of (15), we calculated the E-plane pattern of the antenna with its parameters given as $a = 0.54\ \lambda$, $b = 0.12\ \lambda$, $w = 0.04\ \lambda$, $l = 0.5\ \lambda$, $h = 0.987\ \lambda_0$, $\varepsilon_r = 1.0$, and an operating frequency of $f_r = 4$ GHz. The results are seen in Figure 9 which show a nondegraded beam that has scanned to $\theta_p = 52°$. The results for the broadside radiation ($h = 0.533$) are also included for illustration purposes.

5. CONCLUSIONS

We have presented a complete analysis of a 3-dimensional periodic planar array patch antenna. The finite integration technique (FIT) was used to obtain theoretical results. The adequacy and accuracy of our approach were verified by computing antennas radiation pattern and S_{11} parameter and comparing results with their corresponding measured values. Excellent agreements were observed. We then studied the effects of different antenna parameters such as substrate height and permittivity, array periodicity, patch dimensions and frequency on both broadside, and scanned-beam patterns. This study confirms the beam scanning properties of these antennas. The substrate thickness and its dielectric constant play a major role in determining the beam angle. Based on our analysis, some empirical design rules are given which should be of interest to practical patch antenna designers who would want to avoid extensive numerical analysis.

REFERENCES

[1] A. Sommerfeld, "Fortpflanzung electrodynamischer Wellen an einem zylindrischen Leiter," *Annalen der Physik und Chemie*, vol. 67, pp. 233–290, 1899.

[2] W. Menzel, "A new traveling-wave antenna in microstrip," *Archiv fur Elektronik und Übertragungstechnik*, vol. 33, no. 4, pp. 137–140, 1979.

[3] A. A. Oliner and K. S. Lee, "Microstrip leaky-wave strip antennas," in *Proceedings of IEEE Antennas and Propagation Society International Symposium*, vol. 24, pp. 443–446, Philadelphia, Pa, USA, June 1986.

[4] M. Guglielmi and D. R. Jackson, "Broadside radiation from periodic leaky-wave antennas," *IEEE Transactions on Antennas and Propagation*, vol. 41, no. 1, pp. 31–37, 1993.

[5] P. Burghignoli, G. Lovat, and D. R. Jackson, "Analysis and optimization of leaky-wave radiation at broadside from a class of 1-D periodic structures," *IEEE Transactions on Antennas and Propagation*, vol. 54, no. 9, pp. 2593–2604, 2006.

[6] D. R. Jackson and N. G. Alexopoulos, "Gain enhancement methods for printed circuit antennas," *IEEE Transactions on Antennas and Propagation*, vol. 33, no. 9, pp. 976–987, 1985.

[7] H. Y. Yang and N. G. Alexopoulos, "Gain enhancement methods for printed circuit antennas through multiple superstrates," *IEEE Transactions on Antennas and Propagation*, vol. 35, no. 7, pp. 860–863, 1987.

[8] D. R. Jackson, A. A. Oliner, and A. IP, "Leaky-wave propagation and radiation for a narrow-beam multiple-layer dielectric structure," *IEEE Transactions on Antennas and Propagation*, vol. 41, no. 3, pp. 344–348, 1993.

[9] T. Zhao, D. R. Jackson, J. T. Williams, H.-Y. D. Yang, and A. A. Oliner, "2-D periodic leaky-wave antennas—part I: metal patch design," *IEEE Transactions on Antennas and Propagation*, vol. 53, no. 11, pp. 3505–3514, 2005.

[10] T. Weiland, "Time domain electromagnetic field computation with finite difference methods," *International Journal of Numerical Modelling: Electronic Networks, Devices and Fields*, vol. 9, no. 4, pp. 295–319, 1996.

[11] J.-P. Berenger, "A perfectly matched layer for the absorption of electromagnetic waves," *Journal of Computational Physics*, vol. 114, no. 2, pp. 185–200, 1994.

[12] H. A. Kalhor and M. R. Zunoubi, "Accurate analysis of practical diffraction gratings," in *Proceedings of Progress in Electromagnetics Research Symposium (PIERS '06)*, Tokyo, Japan, August 2006.

[13] M. R. Zunoubi and H. A. Kalhor, "Theoretical and experimental analysis of practical 3-D periodic leaky-wave slot antennas," in *Proceedings of the Mediterranean Microwave Sympsium (MMS '06)*, pp. 72–75, Genova, Italy, September 2006.

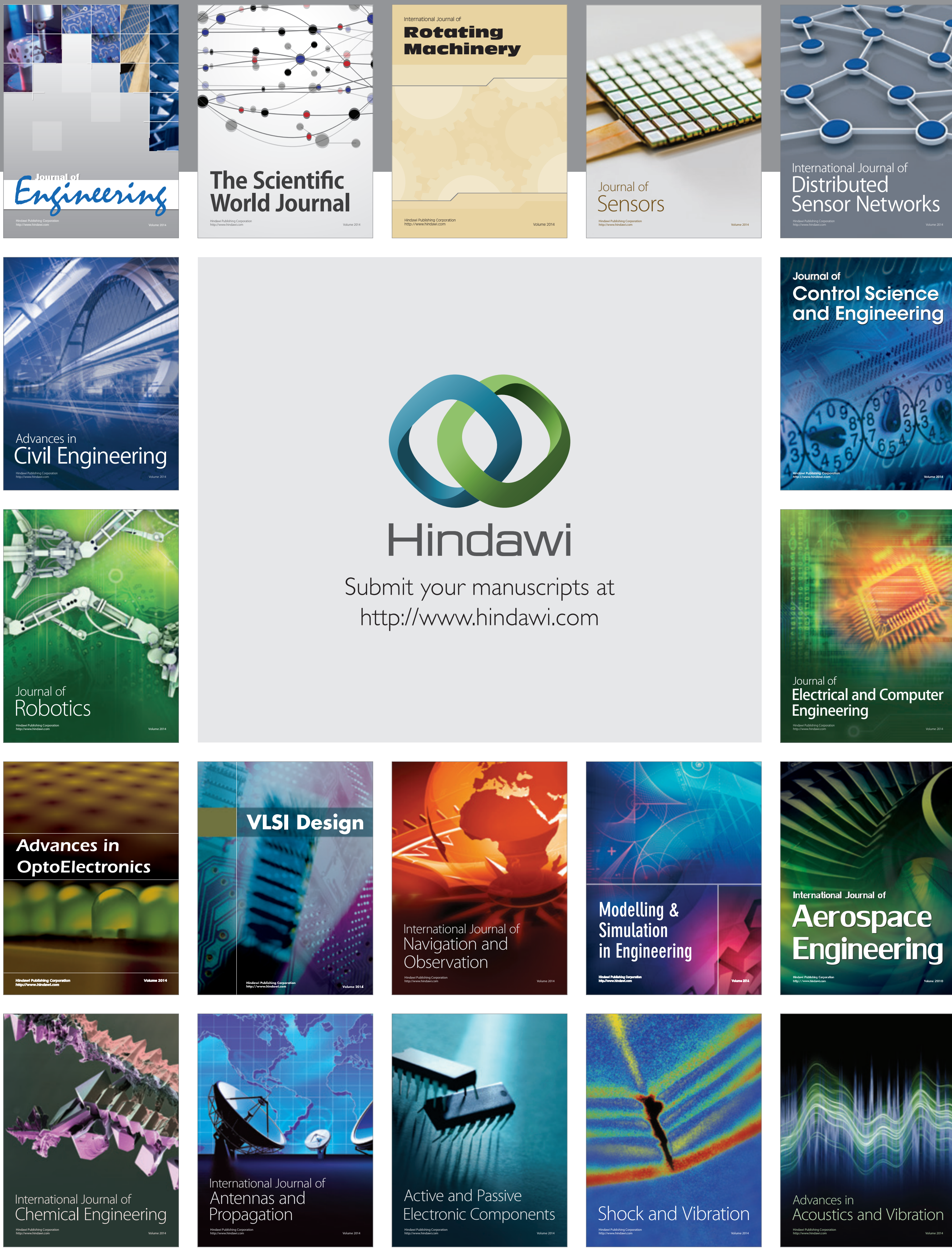
Journal of Engineering
The Scientific World Journal
International Journal of Rotating Machinery
Journal of Sensors
International Journal of Distributed Sensor Networks
Advances in Civil Engineering
Journal of Control Science and Engineering
Hindawi
Submit your manuscripts at
http://www.hindawi.com
Journal of Robotics
Journal of Electrical and Computer Engineering
Advances in OptoElectronics
VLSI Design
International Journal of Navigation and Observation
Modelling & Simulation in Engineering
International Journal of Aerospace Engineering
International Journal of Chemical Engineering
International Journal of Antennas and Propagation
Active and Passive Electronic Components
Shock and Vibration
Advances in Acoustics and Vibration